

Superconductivity in the η -carbide-type oxides $\text{Zr}_4\text{Rh}_2\text{O}_x$

KeYuan Ma^a, Jorge Lago^{a,b}, Fabian O. von Rohr^a

^aDepartment of Chemistry and Department of Physics, University of Zurich, CH-8057 Zürich, Switzerland

^bDepartment of Inorganic Chemistry, Univ. del Pais Vasco (UPV-EHU), 48080 Bilbao, Spain

Abstract

We report on the synthesis and the superconductivity of $\text{Zr}_4\text{Rh}_2\text{O}_x$ ($x = 0.4, 0.5, 0.6, 0.7, 1.0$). These compounds crystallize in the η -carbide structure, which is a filled version of the complex intermetallic Ti_2Ni structure. We find that in the system $\text{Zr}_4\text{Rh}_2\text{O}_x$, already a small amount ($x \geq 0.4$) of oxygen addition stabilizes the η -carbide structure over the more common intermetallic CuAl_2 structure-type, in which Zr_2Rh crystallizes. We show that $\text{Zr}_4\text{Rh}_2\text{O}_{0.7}$ and $\text{Zr}_4\text{Rh}_2\text{O}$ are bulk superconductors with critical temperatures of $T_c \approx 2.8$ K and 4.7 K in the resistivity, respectively. Our analysis of the superconducting properties reveal both compounds to be strongly type-II superconductors with critical fields up to $\mu_0 H_{c1}(0) \approx 8.8$ mT and $\mu_0 H_{c2}(0) \approx 6.08$ T. Our results support that the η -carbides are a versatile family of compounds for the investigation of the interplay of interstitial doping on physical properties, especially for superconductivity.

Keywords: oxides, carbides, η -carbides, superconductivity, intermetallics, Ti_2Ni -structure, CuAl_2 -structure

1. Introduction

A promising approach for superconductivity has been the exploration of layered or cage structured compounds with inter-layer or void positions that can be occupied with additive elements as electron dopants [1]. Most prominently, superconductivity with a critical temperature of $T_c \approx 4$ K was for example discovered in layered Cu_xTiSe_2 via the incorporation of copper between the TiSe_2 layers [2]. In these materials, the addition of copper suppresses a charge-density wave transition and a new superconducting state emerges. An example of a cage structured material in which superconductivity is enhanced, is the compound $\text{Nb}_5\text{Ir}_3\text{O}$ with a critical temperature of $T_c \approx 10.5$ K [3]. In this material oxygen acts as a dopant into the confacial trigonal antiprismatic channels of the Mn_5Si_3 -type structure. Filling these crystallographic spaces with foreign oxygen atoms serves to modify the band topology and increase the superconducting transition temperature.

The here investigated class of compounds crystallize in the so-called η -carbide structure, which is named after its first representatives $\text{Fe}_3\text{W}_3\text{C}$ and $\text{Fe}_4\text{W}_2\text{C}$ [4, 5]. Compounds with this structure are commonly also referred to as E9₃ phases [6]. η -carbides are hard and brittle intermetallic materials that exist for a range of compositions and non-stoichiometries [7, 8, 9, 10]. These compounds crystallize in the cubic space group $Fd\bar{3}m$ and they commonly form for the compositions $\text{A}_3\text{B}_3\text{X}_{1-\delta}$ and $\text{A}_4\text{B}_2\text{X}_{1-\delta}$ with A and B being transition metals, and X being carbon, nitrogen, or oxygen [7]. They consist of a three dimensional metal network on a pyrochlore-type lattice nested by tetrahedrons. This structural feature is commonly referred to as *stella quadrangula*. These super-tetrahedra share vertices to form an infinite diamondoid-like network [6, 10, 11]. The prototypical Ti_2Ni structure has a large face-centered-cubic (fcc) unit cell that contains 96 metallic atoms occupying the

three inequivalent *Wyckoff* 16*d*, 32*e*, and 48*f* positions. The large unit cell of Ti_2Ni consists of eight cubic sub-cells having two alternating patterns, and the interstitial positions between these sub-cells are unoccupied (see, e.g., reference [10]). The η -carbide structure can be understood as a filled version of the Ti_2Ni structure, where the light nonmetallic atoms occupy the 16*c* *Wyckoff* position. Therefore, the transition from the Ti_2Ni structure to the η -carbide structure corresponds to a filling of the cage structured material. This results in a system with tunable crystal and composition chemistry, which create opportunities to modify the properties of these materials by doping interstitial atoms on this 16*c* position.

About 120 compounds are known that crystallize in the η -carbide-type structure (see, e.g. reference [12]). Only few of these compounds have been investigated for their physical properties. Recently, a wide variety of magnetic orderings have been reported in this structure type, such as magnetic frustration, ferromagnetism, and strong magnetic correlations [13, 14, 15, 16, 17, 18]. Known η -carbide-type oxides are $\text{T}_3\text{M}_3\text{O}$ with $T(16d, 32e) = \text{Mn, Fe, Co, Ni}$ and $M = \text{Mo, W, Zr}$, $\text{Zr}_3\text{T}_3\text{O}$ with $T(16d, 32e) = \text{V, Cr, Mn}$, and $\text{M}_4\text{T}_2\text{O}$ with $T = \text{Fe, Ni, and Re}$, $M = \text{Zr, Nb, and Ta}$ [19, 20, 21, 22].

A few compounds with the η -carbide-type structure were reported to be superconductors with critical temperatures up to $T_c \approx 9$ K [22, 23]. Earlier reports on the superconductivity in these materials, however, lack generally a detailed characterization of the chemical structure and purity, as well as the physical properties in both the superconducting and the normal state.

Here, we report on the superconductivity in the η -carbides $\text{Zr}_4\text{Rh}_2\text{O}_{0.7}$ and $\text{Zr}_4\text{Rh}_2\text{O}$ with a maximal critical temperature $T_c \approx 4.7$ K. We find that these are bulk superconductor, with a variable critical temperature depending on the oxygen content. Temperature-dependent magnetic susceptibility, electrical

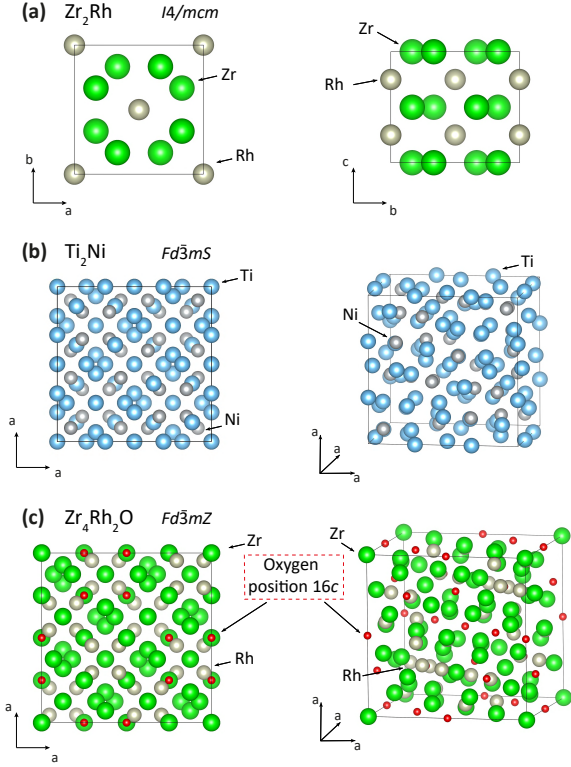


Figure 1: Crystal structures of (a) Zr_2Rh , (b) Ti_2Ni , and $\text{Zr}_4\text{Rh}_2\text{O}$. The structure of $\text{Zr}_4\text{Rh}_2\text{O}$ clearly differs from the structure of the intermetallic phase Zr_2Rh , it can be interpreted as a filled version of the Ti_2Ni structure.

transport and specific heat measurements were used to characterize the superconductors. Our findings show that earlier reports of a critical temperature of $T_c \approx 12$ K in the system Zr-Rh-O cannot be attributed to compounds with the η -carbide structure (see reference [22]). Our results support that the η -carbides are a versatile family of compounds for the investigation of the interplay of interstitial doping on physical properties, especially for superconductivity.

2. Experimental

Polycrystalline samples of $\text{Zr}_4\text{Rh}_2\text{O}_x$ with $x = 0.4, 0.5, 0.6, 0.7$, and 1.0 were prepared from mixtures of zirconium sponge (99.5%, Alfa Aesar), zirconium (IV) oxide (ZrO_2) powder (99.995%, Sigma-Aldrich) and rhodium powder (99.8%, Strem Chemicals, Inc.). Stoichiometric mixture of the starting materials were pressed into pellets. These were melted in an arc furnace in a purified argon atmosphere on a water-cooled copper plate.

The samples were molten 10 times in order to assure the optimal homogeneity of the products, which have high melting points. Subsequently, the solidified melt was carefully ground to a fine powder and pressed into a pellet. The pellet was sealed in a quartz tube with 1/3 atm argon and heated in a furnace for 10 days. The samples with an oxygen content with less than $x \leq 0.7$ were annealed at 1000°C , whereas samples with an oxygen content of more than $x > 0.7$ were annealed at 800°C .

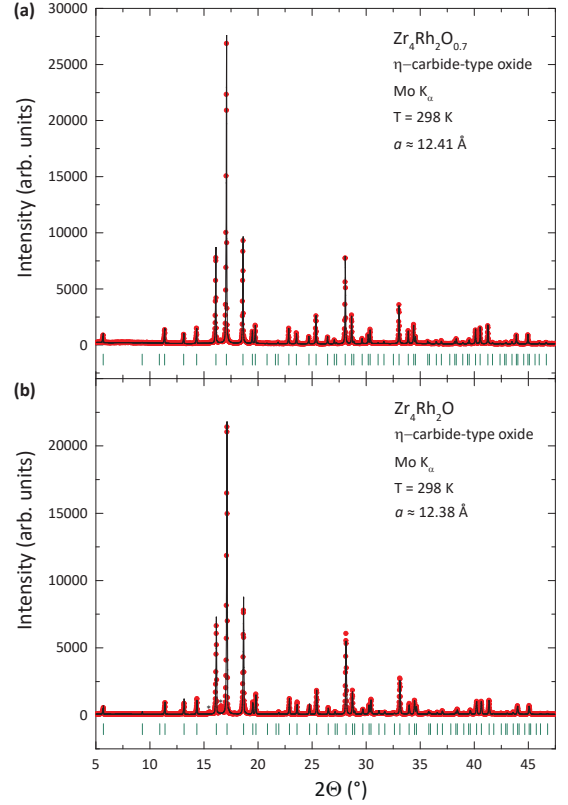


Figure 2: PXRD pattern (red points) at ambient temperature with *LeBail* fits (black line) of the samples with the nominal compositions (a) $\text{Zr}_4\text{Rh}_2\text{O}_{0.7}$ and (b) $\text{Zr}_4\text{Rh}_2\text{O}$. The vertical dark green lines show the theoretical *Bragg* peak positions of the η -carbide-type phase. For $\text{Zr}_4\text{Rh}_2\text{O}$ the broad impurity reflections of Zr_2Rh are marked with a star.

The crystal structure and phase purity of the samples were investigated by powder x-ray diffraction (PXRD) measurements on a STOE STADIP diffractometer with $\text{Mo K}\alpha$ radiation ($\lambda = 0.70930 \text{ \AA}$). The PXRD patterns were collected in the 2θ range of 5 - 50° with a scan rate of $0.25^\circ/\text{min}$. *LeBail* fits were performed using the FULLPROF program package.

The temperature- and field-dependent magnetization measurements were performed using a *Quantum Design* magnetic properties measurement system (MPMSXL) with a 7 T magnet equipped with a reciprocating sample option (RSO). The measured plate like samples were placed in parallel to the external magnetic field to minimize demagnetization effects. Specific heat capacity and resistivity measurements were performed with a *Quantum Design* physical property measurement system (PPMS) with a 9 T magnet. The standard four-probe technique was employed to measure the electrical resistivity with an excitation current of $I = 1.5 \text{ mA}$. In the resistivity measurement, gold wires were connected to the sample with silver paint.

3. Results and Discussion

Crystal Structure. In figure 1(a)-(c), we show a schematic view of the crystal structures of Zr_2Rh , Ti_2Ni , and the η -carbide $\text{Zr}_4\text{Rh}_2\text{O}$. The compound Zr_2Rh crystallizes in the common binary intermetallic structure-type CuAl_2 , generated by square-

triangle nets of atoms, with the body-centered tetragonal space group $I4/mcm$. The compound Ti_2Ni crystallizes in its own cubic structure-type with space group $Fd\bar{3}m$. The coordination number of all atoms in this structure-type is 12, whereas the nickel atoms on the *Wyckoff* position $32e$ arrange on regular tetrahedra, while the titanium atoms on the *Wyckoff* position $48f$ form regular octahedra. The close relationship between the Ti_2Ni structure, the Cr_{23}C_6 , and the η -carbide structure, which has the same metal matrix organization as Ti_2Ni , is depicted in figure 1(b)&(c). An important factor of the Ti_2Ni and the Cr_{23}C_6 structure, respectively, is the ability to dissolve light nonmetallic atoms such as carbon, nitrogen, oxygen, or hydrogen in the interstitial positions. The incorporated interstitial atoms can affect the properties of the compounds drastically. The ideal fully stoichiometric η -carbide $\text{Zr}_4\text{Rh}_2\text{O}$ has a cubic structure adopting the space group $Fd\bar{3}m$, with four distinct atoms sites with the *Wyckoff* positions $48f$, $32e$, $16d$, and $16c$. The zirconium atoms occupy the $16d$ site and the rhodium atoms are in the $32e$ position forming a network of tetrahedra, while zirconium atoms in the $48f$ site form a network of octahedra in which every second one is slightly distorted. These octahedra are connected by sharing faces. The oxygen atoms fill up the interstitial position $16c$ and play a crucial role in stabilizing the ternary η -carbide structure, rather than the for Zr_2Rh reported intermetallic CuAl_2 -type structure.

The room-temperature PXRD pattern and the corresponding *LeBail* fits of polycrystalline samples of the nominal compositions $\text{Zr}_4\text{Rh}_2\text{O}$ and $\text{Zr}_4\text{Rh}_2\text{O}_{0.7}$ are shown in figure 2. The results for $x = 0.4, 0.5$, and 0.6 are shown in the Supplemental Information. All PXRD pattern can be indexed with the η -carbide structure (green vertical tick marks) as the main phase and a CuAl_2 -type structure corresponding to Zr_2Rh as a minor impurity phase. Interestingly, already small oxygen contents, e.g. for $\text{Zr}_4\text{Rh}_2\text{O}_{0.4}$, stabilize the η -carbide-type structure, which is of considerably higher complexity than the CuAl_2 -type structure.

Furthermore, it is noteworthy that no zirconium oxide, especially no Zr(IV) oxide ZrO_2 , was observed as an impurity for any of the samples. The reflections from Zr_2Rh decrease for increasing oxygen contents of the nominal compositions. Compared with other samples, the stoichiometry of $\text{Zr}_4\text{Rh}_2\text{O}_{0.7}$ displays the highest phase purity, with almost no detectable impurity peaks. We observe the lattice parameter a of the η -carbide-type phase to change only slightly for the different samples. The slight decrease of the cell parameter a might be associated to a slight decreasing of the interstitial voids due to enhanced chemical bonding by the addition of the oxygen atoms. A similar behavior was observed in the filled Mn_5Si_3 -type oxides $\text{Nb}_5\text{Ir}_3\text{O}$ and $\text{Zr}_5\text{Pt}_3\text{O}$ [1, 24]. The cell parameter of the *LeBail* fits, the χ^2 and the R_{exp} -values of the fits (both measures for the validity of the structural model) with a model consisting of the two phases Zr_2Rh and an η -carbide are summarized in table 1. Attempts to prepare η -carbides with a stoichiometry of $\text{A}_3\text{B}_3\text{X}_{1-\delta}$, where the $48f$ *Wyckoff* position is occupied by the transition metal B , i.e. rhodium, did not yield any η -carbide-type structures for all tested compositions and synthesis temperatures. Instead we have obtained mixtures

of rocksalt-type ZrRh and the starting materials for all our attempts on this stoichiometry.

Magnetic Properties. In figure 3(a), we show the temperature-dependent magnetization of $\text{Zr}_4\text{Rh}_2\text{O}_{0.7}$ and $\text{Zr}_4\text{Rh}_2\text{O}$ measured in zero-field cooled (ZFC) and field-cooled (FC) mode in an external magnetic field of $\mu_0 H = 2$ mT. Both samples are found to have a diamagnetic shielding fractions corresponding to a bulk superconductor, i.e. $\chi > -1$. Subsequently, the magnetization curves are normalized by plotting the data as $-M(T)/M(1.75 \text{ K})$ for better comparability. We find a superconducting transition temperature of $T_c \approx 2.6 \text{ K}$, and 4.3 K , in the magnetization for $\text{Zr}_4\text{Rh}_2\text{O}_{0.7}$ and $\text{Zr}_4\text{Rh}_2\text{O}$, respectively.

The temperature-dependent magnetization ($M(T)/H$) in zero-field cooled (ZFC) mode in an external magnetic field of $\mu_0 H = 2$ mT of the samples with $x = 0.4, 0.5, 0.6, 0.7$, and 1.0 between $T = 1.75 \text{ K}$ to 8 K are shown in the Supplemental Information. They all show single superconducting transitions with critical temperatures between $T_c \approx 4.3 \text{ K}$ and 2.5 K , with the highest T_c observed for the sample $\text{Zr}_4\text{Rh}_2\text{O}$. All samples are bulk superconductors with diamagnetic shielding fraction larger than -1 . In the Supplemental Information the temperature-dependent magnetization between $T = 10 \text{ K}$ to 300 K for $\text{Zr}_4\text{Rh}_2\text{O}$ in an external field of $\mu_0 H = 0.1 \text{ T}$ is shown. We find, $\text{Zr}_4\text{Rh}_2\text{O}$ to be a Pauli paramagnetic metal in the normal state, with little temperature-dependence of the magnetization.

In figure 3(b), we show the ZFC field-dependent magnetization $m(H)$ in fields between $\mu_0 H = 0$ to 25 mT for temperatures between $T = 1.75$ to 4 K (in 0.25 K steps). It is well-known to be challenging to extract precise values for the lower critical field H_{c1} from $m(H)$ measurements, especially for polycrystalline samples. As a criterion, we have here used the identification of H_{c1} as the magnetic field where $m(H)$ first deviates from linearity. The extracted H_{c1} values are plotted in the inset of figure 3(b). A reasonable estimate for $H_{c1}(0)$ can then be obtained by using the following empirical formula [25]

$$H_{c1}(T) = H_{c1}(0)[1 - (T/T_c)^2]. \quad (1)$$

With this approximation, we obtain a lower critical field of $\mu_0 H_{c1}(0) \approx 8.8 \text{ mT}$. This value is in good agreement with similar superconducting materials.

Electrical Transport. The temperature-dependent electrical resistivity $\rho(T)$ in zero-field of polycrystalline samples of $\text{Zr}_4\text{Rh}_2\text{O}_{0.7}$ and $\text{Zr}_4\text{Rh}_2\text{O}$ are presented in figure 4(a)&(b). The room temperature resistivities of the two compounds are $\rho(300\text{K}) = 0.11 \text{ m}\Omega \text{ cm}$ and $0.23 \text{ m}\Omega \text{ cm}$, respectively. With decreasing temperature, the resistivity decreases only slightly with a nearly linear temperature dependence of

$$\rho = \rho_0 + \beta T. \quad (2)$$

Here, ρ_0 is the residual resistivity, revealing a metallic behavior with a low room temperature resistivity value in the normal state of $\rho_0 = 0.10 \text{ m}\Omega \text{ cm}$ for $\text{Zr}_4\text{Rh}_2\text{O}_{0.7}$, and $\rho_0 = 0.14 \text{ m}\Omega \text{ cm}$ for $\text{Zr}_4\text{Rh}_2\text{O}$, respectively. The residual resistivity ratio (RRR) value for $\text{Zr}_4\text{Rh}_2\text{O}_{0.7}$ is $\text{RRR} = \rho(300 \text{ K})/\rho(5 \text{ K}) \approx 1.08$, and

Nominal Compositions	Zr ₄ Rh ₂ O _{0.4}	Zr ₄ Rh ₂ O _{0.5}	Zr ₄ Rh ₂ O _{0.6}	Zr ₄ Rh ₂ O _{0.7}	Zr ₄ Rh ₂ O
cell parameter a [Å]	12.41270(6)	12.40608(5)	12.40143(3)	12.41014 (3)	12.38112 (8)
Quality of the <i>LeBail</i> fit χ^2	7.61	5.55	2.85	3.74	9.75
Quality of the <i>LeBail</i> fit R_{exp}	8.99	8.94	10.54	7.89	7.91

Table 1: Cell parameters a of the prepared samples with the nominal compositions Zr₄Rh₂O _{x} with $x = 0.4, 0.5, 0.6, 0.7$, and 1.0, and the quality of the refinements of the performed *LeBail* fits with a model consisting of the two phases Zr₂Rh and an η -carbide.

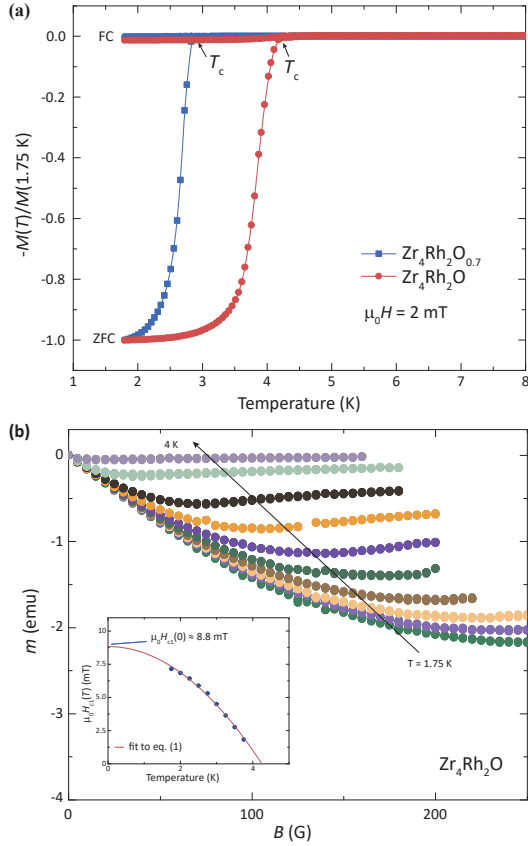


Figure 3: (a) ZFC and FC magnetization of Zr₄Rh₂O_{0.7} and Zr₄Rh₂O in an external field of $\mu_0 H = 2$ mT between $T = 1.75$ K to 8 K. In the inset, the temperature-dependent magnetization between $T = 10$ K to 300 K in an external field of $\mu_0 H = 1$ T is shown. (b) Field-dependent magnetization of Zr₄Rh₂O between $T = 1.75$ K to 4 K in 0.25 T steps in low fields $\mu_0 H < 25$ mT in order to determine the lower critical field H_{c1} . The inset shows the temperature dependence of the lower critical field H_{c1} of Zr₄Rh₂O.

Zr₄Rh₂O is $\text{RRR} = \rho(300 \text{ K})/\rho(5 \text{ K}) \approx 1.62$. The RRR values and the absolute values of resistivity indicating that Zr₄Rh₂O is slightly more metallic than Zr₄Rh₂O_{0.7}. The values are, however, similar for both. They correspond to poor metals and are especially for intermetallics with substantial covalent bonding and for metallic oxides (see, e.g., references [26, 27]).

Both compounds show distinct transitions to a superconducting state in the resistivity at critical temperatures of $T_c = 2.8$ K for Zr₄Rh₂O_{0.7} and $T_c = 4.7$ K for Zr₄Rh₂O, respectively. These values are slightly higher, and therefore in good agreement with the values obtained from the magnetization measurements. In the inset of figures 4(a)&(b), the normalized resistivities $\rho(T)/\rho(6 \text{ K})$ in external magnetic fields between $\mu_0 H = 0$ T to 5 T and 7 T, restrictively, are shown. As expected for type-II superconductors, the critical temperature decreases steadily as the applied magnetic field increases for both samples.

In order to determine the upper critical fields $H_{c2}(0)$ the commonly used 50% criterion was applied, which corresponds to the midpoints of resistances (see, e.g. references [28, 29, 30]). The obtained values are plotted in figure 4(c). The extrapolated slopes near T_c are $dH_{c2}/dT = -2.51(6)$ T/K for Zr₄Rh₂O_{0.7}, and $dH_{c2}/dT = -1.95(2)$ T/K for Zr₄Rh₂O. From these slopes, we can make a conservative evaluation of the upper critical fields at zero temperature $H_{c2}(0)$ using the Werthamer-Helfand-Hohenberg (WHH) approximation in the dirty limit, according to [31]:

$$H_{c2}^{\text{WHH}}(0) = -0.693 T_c \left(\frac{dH_{c2}}{dT} \right)_{T=T_c}. \quad (3)$$

The resulting upper critical fields are $\mu_0 H_{c2}(0) \approx 4.87$ T for Zr₄Rh₂O_{0.7}, and $\mu_0 H_{c2}(0) \approx 6.35$ T for Zr₄Rh₂O, respectively. Both upper critical fields are lower than, and therefore in agreement with the Pauli paramagnetic limit, where $\mu_0 H_{\text{Pauli}} = 1.85 \cdot T_c = 5.18$ T for Zr₄Rh₂O_{0.7}, and $\mu_0 H_{\text{Pauli}} = 8.70$ T for Zr₄Rh₂O.

The above determined critical fields $H_{c1}(0)$ and $H_{c2}(0)$ can be used to calculate several other superconducting parameters. According to Ginzburg-Landau theory, the upper critical field at $T = 0$ K, $H_{c2}(0)$, can be used to estimate the coherence length $\xi(0)$ according to the expression

$$\mu_0 H_{c2}(0) = \frac{\Phi_0}{2\pi \xi(0)^2}. \quad (4)$$

Here, $\Phi_0 = h/(2e) \approx 2.0678 \cdot 10^{-15}$ Wb is the magnetic flux quantum. The resulting coherence lengths for Zr₄Rh₂O_{0.7} is

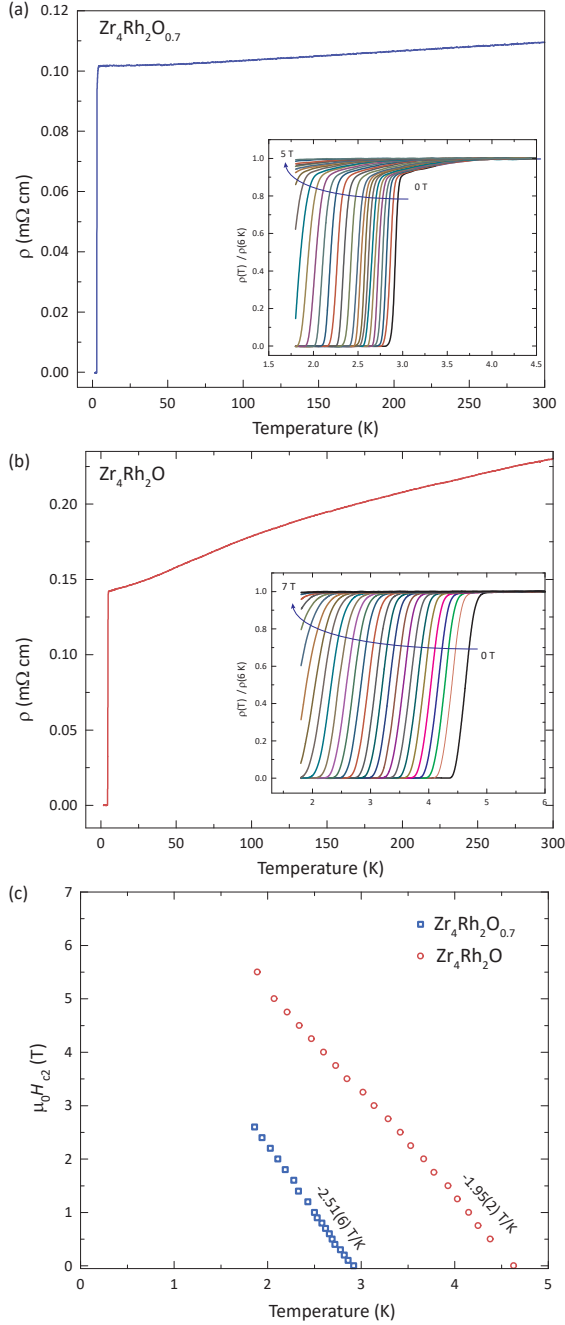


Figure 4: (a)&(b) Temperature-dependent resistivities in zero field of $\text{Zr}_4\text{Rh}_2\text{O}_{0.7}$ and $\text{Zr}_4\text{Rh}_2\text{O}$ between $T = 300$ K to 1.8 K, respectively. The insets show the normalized resistivities $\rho(T)/\rho(6\text{ K})$ in the vicinity of the superconducting transition and in external fields between $B = 0$ T to 7 T in 0.5 T steps. (c) Upper critical fields of $\text{Zr}_4\text{Rh}_2\text{O}_{0.7}$ and $\text{Zr}_4\text{Rh}_2\text{O}$ determined by the 50% criterion from the data shown in the insets of (a)&(b).

Parameters	$\text{Zr}_4\text{Rh}_2\text{O}_{0.7}$	$\text{Zr}_4\text{Rh}_2\text{O}$
$T_{c,\text{magnetization}}$ [K]	2.6	4.3
$T_{c,\text{resistivity}}$ [K]	2.8	4.7
$T_{c,\text{specificheat}}$ [K]	2.7	4.1
$\rho(300\text{ K})$ [m Ω cm]	0.11	0.23
RRR	1.08	1.62
$H_{c1}(0)$ [mT]	-	8.8
$H_{c2}(0)$ [T]	4.89	6.08
β [mJ mol $^{-1}$ K $^{-4}$]	1.43	2.01
γ [mJ mol $^{-1}$ K $^{-2}$]	14.5	17.9
Θ_D [K]	209	189
$\xi(0)$ [Å]	83	72
$\lambda(0)$ [Å]	-	3199
$\mu_0 H_c$ [mT]	-	101
$\Delta C/\gamma T_c$	2.25	1.74
$\lambda_{\text{el-ph}}$	0.60	0.73
$\Delta(0)$ [meV]	0.47	0.64

Table 2: Summary of the superconducting and normal state parameters of $\text{Zr}_4\text{Rh}_2\text{O}_{0.7}$ and $\text{Zr}_4\text{Rh}_2\text{O}$.

$\xi(0) = 82$ Å, and $\xi(0) = 73$ Å for $\text{Zr}_4\text{Rh}_2\text{O}$, respectively.

The here obtained values clearly indicate that these η -carbide-type oxides must be strongly type-II superconductors with a Ginzburg-Landau parameter of the order of $\kappa = \lambda/\xi \approx 44$ for $\text{Zr}_4\text{Rh}_2\text{O}$. Type-II superconductors need to have a value for $\kappa > 1/\sqrt{2}$. Ginzburg-Landau parameter is estimated from the above obtained values for $H_{c1}(0)$ and $\xi(0)$ by using the relations [25]:

$$\mu_0 H_{c1} = \frac{\phi_0}{4\pi\lambda^2} \ln\left(\frac{\kappa}{\xi}\right), \quad (5)$$

With this relations we find a value of $\lambda \approx 3199$ Å for $\text{Zr}_4\text{Rh}_2\text{O}$. Combining the results of $H_{c1}(0)$, $H_{c2}(0)$ and κ the thermodynamic critical field H_c can be estimated according to

$$H_{c1} \cdot H_{c2} = H_c \ln(\kappa^2). \quad (6)$$

This calculation yields $\mu_0 H_c \approx 101$ mT for $\text{Zr}_4\text{Rh}_2\text{O}$.

Specific Heat. In figure 5 the temperature-dependent specific heat capacities $C(T)$ of $\text{Zr}_4\text{Rh}_2\text{O}_{0.7}$ and $\text{Zr}_4\text{Rh}_2\text{O}$ are depicted in the vicinity of the superconducting transition. The data is plotted in a C/T vs. T representation. The normal-state contribution constitutes above the critical temperature T_c of an electronic (C_{el}) and a phononic (C_{phonon}) contribution, and can be fitted according to the expression:

$$\frac{C(T)}{T} = \frac{C_{el} + C_{phonon}}{T} = \gamma + \beta T^2 \quad (7)$$

where γ is the electronic specific heat coefficient and β is the coefficient of the lattice contribution. The resulting values for β are $1.43 \text{ mJ mol}^{-1} \text{ K}^{-4}$ for $\text{Zr}_4\text{Rh}_2\text{O}_{0.7}$ and $2.01 \text{ mJ mol}^{-1} \text{ K}^{-4}$ for $\text{Zr}_4\text{Rh}_2\text{O}$, respectively. The corresponding values for γ are found to be $14.5 \text{ mJ mol}^{-1} \text{ K}^{-2}$ for $\text{Zr}_4\text{Rh}_2\text{O}_{0.7}$ and $17.9 \text{ mJ mol}^{-1} \text{ K}^{-2}$ for $\text{Zr}_4\text{Rh}_2\text{O}$. The Debye temperature Θ_D can be calculated according the following relation:

$$\Theta_D = \left(\frac{12\pi^4}{5\beta} nR \right)^{\frac{1}{3}} \quad (8)$$

where R is the ideal gas constant and n is the number of atoms per formula unit. The resulting *Debye* temperatures are calculated to be $\Theta_D \approx 209 \text{ K}$ for $\text{Zr}_4\text{Rh}_2\text{O}_{0.7}$, and $\Theta_D \approx 189 \text{ K}$ for $\text{Zr}_4\text{Rh}_2\text{O}$. The electronic specific heat (C_{el}) is obtained by subtracting the normal state phononic contribution C_{phonon} from the total specific heat.

The critical temperatures obtained in the specific heat measurements are $T_c \approx 2.7 \text{ K}$ for $\text{Zr}_4\text{Rh}_2\text{O}_{0.7}$ and 4.1 K for $\text{Zr}_4\text{Rh}_2\text{O}$ using an equal-area entropy construction method. These values are in good agreement with the critical temperatures obtained from resistivity and magnetization measurements. The normalized specific heat jump, $\Delta C/\gamma T_c$ is found to be 2.25 for $\text{Zr}_4\text{Rh}_2\text{O}_{0.7}$ and 1.74 for $\text{Zr}_4\text{Rh}_2\text{O}$. Both values are larger than the weak coupling BSC limit of 1.43, verifying the bulk nature of the superconductivity in both compounds.

The electron-phonon coupling constant λ_{el-ph} can be estimated using the *McMillan* formula. This formula is based on the phonon spectrum of niobium [33, 34]. This approximation is valid for $\lambda_{el-ph} < 1.25$ [35]:

$$\lambda_{el-ph} = \frac{1.04 + \mu^* \ln\left(\frac{\Theta_D}{1.45T_c}\right)}{(1 - 0.62\mu^*)\ln\left(\frac{\Theta_D}{1.45T_c}\right) - 1.04} \quad (9)$$

The parameter μ^* is the effective Coulomb repulsion, which arises from Coulomb-coupling propagating much more rapidly than phonon-coupling. For the estimation of the electron-phonon coupling, we are using the common approximation of $\mu^* = 0.13$. This value is an average value, which is valid for many intermetallic superconductors (see, e.g., reference [30, 32]). We obtain electron-phonon coupling constants of $\lambda_{el-ph} \approx 0.60$ for $\text{Zr}_4\text{Rh}_2\text{O}_{0.7}$ and 0.73 for $\text{Zr}_4\text{Rh}_2\text{O}$, respectively. These values suggest that both compounds are weak-coupling superconductor.

From the electronic low temperature specific heat data, we have estimated the value of the superconducting gap $\Delta(0)$ of the two compounds, according to

$$C_{el} = a \exp(-\Delta(0)/k_B T_c). \quad (10)$$

We obtain calculated superconducting gaps of $\Delta(0) \approx 0.47 \text{ meV}$ for $\text{Zr}_4\text{Rh}_2\text{O}_{0.7}$ and 0.64 meV for $\text{Zr}_4\text{Rh}_2\text{O}$, respectively. All superconducting parameters that we have obtained here for $\text{Zr}_4\text{Rh}_2\text{O}_{0.7}$ and $\text{Zr}_4\text{Rh}_2\text{O}$ are summarized in

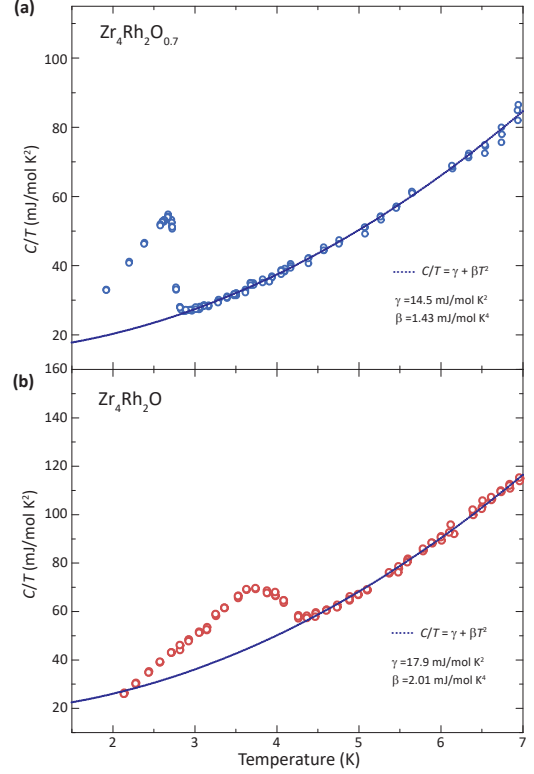


Figure 5: Temperature-dependent specific heat capacities $C(T)$ of (a) $\text{Zr}_4\text{Rh}_2\text{O}_{0.7}$ and (b) $\text{Zr}_4\text{Rh}_2\text{O}$ between $T = 2 \text{ K}$ to 7 K . The data is plotted in a C/T vs. T representation. The dotted line corresponds to a fit of the normal state specific heat capacities, according to equation 7.

table 2.

4. Conclusion

In summary, we have described the successful synthesis of the η -carbides with the nominal compositions $\text{Zr}_4\text{Rh}_2\text{O}_x$ with $x = 0.4, 0.5, 0.6, 0.7$, and 1.0 . We find that already a small addition of oxygen changes the crystal structure from the very common intermetallic CuAl_2 -type to the η -carbide-type structure, which corresponds to a filled version of the Ti_2Ni structure. Nearly phase-pure samples, with the minor impurity phase Zr_2Rh , were obtained for all nominal compositions.

The compounds $\text{Zr}_4\text{Rh}_2\text{O}_{0.7}$ and $\text{Zr}_4\text{Rh}_2\text{O}$ compounds were found to be bulk superconductors with critical temperatures of $T_c \approx 2.8 \text{ K}$ and 4.7 K in the resistivity, respectively. We have characterized the properties of $\text{Zr}_4\text{Rh}_2\text{O}_{0.7}$ and $\text{Zr}_4\text{Rh}_2\text{O}$ in the normal and the superconducting states by magnetization, electrical transport, and specific heat capacity measurements. Both, compounds display a well developed discontinuity in the specific heat of $\Delta C/\gamma T_c \approx 2.25$ for $\text{Zr}_4\text{Rh}_2\text{O}_{0.7}$ and 1.74 for $\text{Zr}_4\text{Rh}_2\text{O}$, respectively, and a large diamagnetic shielding fraction ($\chi > -1$), which confirm the the bulk nature of superconductivity in these materials. We find these η -carbide-type oxides to be strong type-II superconductors with upper critical fields $\mu_0 H_{c2}$ close to the Pauli paramagnetic limit.

Our findings indicate that earlier reports of a critical temperature of $T_c \approx 12$ K in the system Zr-Rh-O cannot be attributed to the η -carbide structure (for the here investigated stoichiometries). But, it is likely that these critical temperatures are rather related to the CuAl_2 -type $\text{Zr}_{2-x}\text{Rh}_x$ alloys (see, e.g., reference [36]). We find the η -carbides to be a versatile family of compounds for the investigation of the interplay of interstitial doping on physical properties, especially for superconductivity.

Acknowledgments

This work was supported by the Swiss National Science Foundation under Grant No. PZ00P2_174015.

References

- [1] H. Hosono, S.-W. Kim, S. Matsuishi, S. Tanaka, A. Miyake, T. Kageyama, K. Shimizu, *Phil. Trans. R. Soc. A* 373 (2015) 20140450.
- [2] E. Morosan, H. W. Zandbergen, B. S. Dennis, J. W. G. Bos, Y. Onose, T. Klimczuk, A. P. Ramirez, N. P. Ong, R. J. Cava, *Nature Physics* 2 (2006) 544.
- [3] Y. Zhang, B. Wang, Z. Xiao, Y. Lu, T. Kamiya, Y. Uwatoko, H. Kageyama, H. Hosono, *npj Quantum Materials* 2 (2017) 45.
- [4] V. Adelsköld, A. Sunderlin, A. Westgren, *Z. anorg. Chem.* 212 (1933) 401.
- [5] A. Westgren, G. Phragmen, *Trans. Amer. Soc. Steel Treat.* 13 (1928) 539.
- [6] H. Nyman, S. Andersson, M. O'Keeffe, *J. Solid State Chem.* 26 (1978) 123.
- [7] L.E. Toth, *Transition Metal Carbides and Nitrides, Refractory Materials*, Academic Press, New York (1971).
- [8] A.C. Fraker, H.H. Stadelmaier, *Trans. Metal. AIME* 245 (1969) 847.
- [9] S.M. Hunter, D. McKay, R.I. Smith, J.S.J. Hargreaves, D.H. Gregory, *Chem. Mater.*, 22 (2010), p. 2898.
- [10] M. Souissi, H.F. Sluiter, T. Matsunaga, M. Tabuchi, M.J. Mills, Ryoji Sahara *Scientific Reports* 8 (2018) 7279.
- [11] L.A. Sviridov, P.D. Battle, F. Grandjean, G.J. Long, T.J. Prior, *Inorg. Chem.* 49 (2010) 1133.
- [12] M. Hellebrandt, *Crystallography Reviews* 10 (2004) 17.
- [13] T. Waki, S. Terazawa, Y. Umemoto, Y. Tabata, Y. Murase, M. Kato, K. Hirota, H. Nakamura, *Journal of Physics: Conference Series* 344 (2012) 01201.
- [14] T. Waki, S. Terazawa, Y. Tabata, F. Oba, C. Michioka, K. Yoshimura, S. Ikeda, H. Kobayashi, K. Ohoyama, H. Nakamura, *J. Phys. Soc. Jpn.* 79 (2010) 043701.
- [15] T. Waki, S. Terazawa, Y. Tabata, Y. Murase, M. Kato, K. Hirota, S. Ikeda, H. Kobayashi, K. Sato, K. Kindo, H. Nakamura, *J. Alloys Comp.* 509 (2011) 9451.
- [16] R.N. Panda, N.S. Gajbhiye, *J. Alloys Comp.* 256 (1997) 102.
- [17] S.K. Jackson, R.C. Layland, H.-C. zur Loye, *J. Alloys Comp.* 291 (1999) 94.
- [18] T.J. Prior, P.D. Battle, *J. Mater. Chem.* 14 (2004) 3001.
- [19] N. Schonberg, *Acta Chem. Scand.* 8 (1954) 932.
- [20] H. Holleck and F. Thummler, *J. Nucl. mater.* 23 (1967) 88.
- [21] H. Holleck and F. Thummler, *Mh. Chemie* 112 (1967) 133.
- [22] B. T. Matthias *et al.*, *Rev. Mod. Phys.* 35 (1963) 1.
- [23] H.C. Ku and D.C. Johnson, *Chinese Journal of Physics* 22 (1984) 59.
- [24] S. Hamamoto and J. Kitagawa, *Mater. Res. Express* 5 (2018) 106001.
- [25] E. H. Brandt, *Phys. Rev. B* 68 (2003) 054506.
- [26] F.O. von Rohr, H. Luo, N. Ni, M. Wörle, and R. J. Cava, *Phys. Rev. B* 89 (2014) 224504.
- [27] F.O. von Rohr, A. Ryser, H. Ji, K. Stolze, J. Tao, J.J. Frick, G.R. Patzke, R.J. Cava, *Chem. Eur. J.* 25 (2019) 2082.
- [28] T.P. Orlando, E.J. McNiff Jr, S. Foner, M. R. Beasley, *Phys. Rev. B* 19 (1979) 4545.
- [29] F. von Rohr, R. Nesper, A. Schilling, *Phys. Rev. B* 89 (2014) 094505.
- [30] F.O. von Rohr, M. Winiarski, J. Tao, T. Klimczuk, R.J. Cava, *Proc. Natl. Acad. Sci.* 113 (2016) E7144.
- [31] N.R. Werthamer, E. Helfand, and P.C. Hohenberg, *Physical Review* 147 (1966) 295.
- [32] T. Klimczuk, C.H. Wang, K. Gofryk, F. Ronning, J. Winterlik, G.H. Fecher, J.-C. Griveau, E. Colineau, C. Felser, J.D. Thompson, D.J. Sarik, R.J. Cava, *Phys. Rev. B* 85 (2012) 174505.
- [33] W.L. McMillan, *Phys. Rev.* 167 (1968) 331.
- [34] R.C. Dynes, *Solid State Commun.* 10 (1972) 615.
- [35] P.B. Allen, R.C. Dynes, *Phys. Rev. B* 12 (1975) 3.
- [36] S.L. McCarthy, *Journal of Low Temperature Physics* 4 (1971) 485.